



ELSEVIER

Biomaterials 21 (2000) 2263–2272

Biomaterials

Correlation of transarterial transport of various dextrans with their physicochemical properties

Omar Elmalak^a, Mark A. Lovich^a, Elazer Edelman^{b,*}

^aHarvard University-Massachusetts Institute of Technology, Division of Health Sciences and Technology, Massachusetts Institute of Technology, Cambridge, MA 02139, USA

^bCardiovascular Division, Department of Internal Medicine, Brigham and Women's Hospital and Harvard Medical Schools, Boston, Massachusetts 02115, USA

Abstract

Local vascular drug delivery provides elevated concentrations of drug in the target tissue while minimizing systemic side effects. To better characterize local pharmacokinetics we examined the arterial transport of locally applied dextran and dextran derivatives *in vivo*. Using a two-compartment pharmacokinetic model to correct the measured transmural flux of these compounds for systemic redistribution and elimination as delivered from a photopolymerizable hydrogel surrounding rat carotid arteries, we found that the diffusivities and the transendothelial permeabilities were strongly dependent on molecular weight and charge. For neutral dextrans, the effective diffusive resistance in the media increased with molecular weight approximately 4.1-fold between the molecular weights of 10 and 282 kDa. Similarly, endothelial resistance increased 28-fold over the same molecular weight range. The effective medial diffusive resistance was unaffected by cationic charge as such molecules moved identically to neutral compounds, but increased approximately 40% when dextrans were negatively charged. Transendothelial resistance was 20-fold lower for the cationic dextrans, and 11-fold higher for the anionic dextrans, when both were compared to neutral counterparts. These results suggest that, while low molecular weight drugs will rapidly traverse the arterial wall with the endothelium posing a minimal barrier, the reverse is true for high molecular weight agents. With these data, the deposition and distribution of locally released vasoactive compounds might be predicted based upon chemical properties, such as molecular weight and charge. © 2000 Elsevier Science Ltd. All rights reserved.

Keywords: Dextran; Two-compartment model; Transarterial transport; Pharmacokinetics; Vascular permeability; Diffusion

1. Introduction

The revascularization of blood vessels beset with atherosclerotic disease with balloon angioplasty or vascular bypass surgery is often accompanied by endothelial and arterial injury resulting in subsequent smooth muscle cell hyperplasia and clinical restenosis [1,2]. One promising solution for this problem is directed or local application of anti-hyperplastic compounds, to provide elevated concentrations in target arterial tissues, while minimizing systemic side effects [3,4]. Polymeric drug release devices can deliver drugs to specific arterial segments from the endovascular or perivascular aspects of blood vessels. Endovascular sustained release has been accomplished from drug eluting expandable stents [5–7]

or from rigid polymeric sheets or hydrogels [8–11]. Perivascular drug delivery can be achieved by releasing drug from polymeric slabs, microspheres or circumferential wraps [3,4,11,12]. The rational design and clinical utility of these local modes of delivery depend on their ability to transfer drug to the target cells within the arterial wall quickly, for sustained durations, and at therapeutic concentrations for biologic effect to emerge [13]. Therefore, careful consideration of the governing mechanisms of transvascular transport of vasoactive agents, such as transendothelial permeability and solute effective diffusivity in arterial media, are warranted.

Previous studies of transvascular transport of solutes have focused on intrinsic plasma-based macromolecules such as low-density lipoproteins [14–17] and serum albumin [18–21]. After decades of research, the diffusive and transendothelial mechanisms of macromolecular transport across the arterial wall are receiving renewed interest with the advent of sustained drug release

*Corresponding author. Tel.: +1-617-253-1569; fax: +1-617-253-2514.

E-mail address: eedelman@mit.edu (E. Edelman).

Nomenclature

| | | | |
|------------------|---|------------------------|---|
| b_{end} | coefficient of endothelial resistance (0, denuded; 1, intact) | l_{med} | the thickness of media |
| C | concentration of either compartment in the pharmacokinetic model (Fig. 1) | P | average perimeter of artery, length of Internal Elastic Lamina |
| C_{gel} | concentration of the perivascular gel | R_{end} | transendothelial resistance to solute transport |
| D_{med} | diffusivity of solute in the arterial media | R_{med} | diffusivity of dextran in the arterial media |
| J_{in} | Transarterial mass transfer rate of solutes | R_{tot} | the total diffusive resistance of the artery to the transmural solute transport |
| k_1, k_2 | first-order rate constants of dextran transfer between central and peripheral compartment | V | volume of either compartment in the pharmacokinetic model (Fig. 1) |
| k_{cl} | first-order rate constant for dextran elimination from the central compartment | λ_1, λ_2 | pharmacokinetic exponential decay constants (Eq. (2)), reflect the distribution and elimination phase, respectively |
| L | length of an artery | | |

technologies and the failure of more accepted systemic modes of delivery to have impact on vascular disease. Vasoactive compounds that have potential in proliferative vascular diseases, however, span a wide range of physicochemical properties, such as molecular weight and charge, and do not generally resemble atherogenic compounds. We therefore sought to correlate independent physico-chemical properties with vascular transport parameters. We measured the effective diffusivity within the arterial media and the transendothelial resistance, in an *in vivo* rat carotid model, for families of dextrans that ranged in molecular weight from 10 to 282 kDa. In addition we correlated these transport parameters with molecular charge using anionic, neutral, and cationic 40 kDa dextrans. We use the term 'effective diffusivity' to describe the observed transport which includes the impact of steric forces, potential specific and nonspecific binding interactions within the tissue interstitium, and cellular internalization, in addition to the diffusive random thermal motion of solutes down concentration gradients. The data obtained may well enable us to describe transvascular transport and predict the arterial distribution after local delivery for any hypothetical vasoactive compound based on its size and charge. Such a tool may well allow us to assess the vascular pharmacokinetics of many current and future vasoactive compounds and guide the development of local drug delivery strategies.

2. Materials and methods

2.1. Synthesis

Dextrans and dextran sulfates were radiolabeled with ^{125}I , using tyramine conjugation and reductive amination [22,23]. Briefly, dextran (25 μeq ; MW 10, 40, 78, and

282 kDa; Sigma, St. Louis, MO) and tyramine (35 mg, 250 μeq , Aldrich) were dissolved in 12 ml of double-distilled water (double-distilled water) (pH 6.5) and heated at 80°C for 3 h. The mixture was cooled to 65°C, 100 μmol of sodium cyanoborohydride (NaCNBH_3 , Aldrich) was added, and incubated at 65°C for performed for 10 h. The solution was diluted 8-fold with double-distilled water and dialyzed against double-distilled water (molecular weight cut-off 2000) for 48 h. The pure dextran-tyramine conjugate was obtained in 60–80% yield after freeze-drying. The tyramine content on each polymeric chain was calculated from UV absorption at 275 nm referenced to calibration curve of free tyramine (model Lambda 20, Perkins Elmer UV/VIES spectrophotometer, Norwalk, CT).

2.1.1. Sulfation

The hydroxyl groups on natural dextran-tyramine conjugates were converted to sulfate groups by the methods of Ricketts et al. [24]. Chlorosulfonic acid (4.4 ml, Aldrich) was added drop wise at -10°C to dry pyridine (40 ml, Aldrich) and stirred for 30 min. The temperature was raised to 65°C and the tyramine-dextran 40 kDa (2 g, 37 meq) was added with 5 ml of formamide (Aldrich) dispersed in the reaction mixture by vigorous stirring for 4 h at 65°C. The mixture was neutralized with 0.1 N NaOH and precipitated with 200 ml of ethyl alcohol. The gummy product was purified by dissolution in double-distilled water, neutralized again and dialyzed against double-distilled water (molecular weight cut-off 8000) for 48 h. The degree of sulfation was governed by the reaction time and amount of chlorosulfonic acid.

2.1.2. DMEDA-dextrans

Cationic dextrans were prepared in a two-step process based on the method of Bernstein et al. [25] which

involved oxidation of native dextran with sodium periodate followed by reaction of the polyaldehyde derivative with (DMEDA) and tyramine. Sodium periodate (Aldrich) was dissolved in 500 ml double-distilled water (0.03 M), and dextran (10 g, 40 kDa) was added. The mixture was stirred at room temperature for 3 h in the dark. The clear solution was dialyzed against double-distilled water (molecular weight cut-off 8000) for 48 h and then freeze-dried. The degree of oxidization was determined by measuring the formed aldehydes in the following manner: the polyaldehyde dextran was reacted with an excess of hydroxylamine hydrochloride and the amount of HCl released was measured by titration with 0.1 N NaOH [26]. The second step was the reductive amination of the oxidized dextran with tyramine and *N,N*-dimethylethylenediamine (DMEDA, Aldrich). Briefly, oxidized dextran (1 g) and 50 mg of tyramine were dissolved and mixed in double-distilled water (100 ml) for 30 min at room temperature and then DMEDA (7 ml) was added. The reaction mixture was stirred for 5 h at room temperature followed by the addition of 1 g of NaCNBH₃. The mixture was incubated for additional 6 h, and then purified as above.

The molecular weights of all of the products (dextran, dextran Sulfate, and DMEDA-dextran) were determined relative to PEO standards in sodium nitrate buffer (0.01 M, 10 mg/ml) by gel permeation chromatography (GPC) on a Hewlett Packard Series 1100 chromatograph with a refractive index Optilab detector (Wyatt Technology, Santa Barbara, CA). All products were also analyzed by UV spectroscopy to determine the tyramine content, and elemental analysis (Galbraith Laboratories, Inc.). To determine the density of the charge on the polymeric chain charged dextrans were run on isoelectric focusing (IEF) gels and compared to IEF standards (Bio-Rad).

2.1.3. Radiolabeling dextrans

The pure dextran-tyramine derivatives were radiolabeled with ¹²⁵I using IODO-BEADS. Briefly, for each iodination, 50 mg of dextran derivative at a concentration of 0.5 g/ml was iodinated with 2 IODO-BEADS (Pierce, Rockford, IL) and 2 mCi Na-¹²⁵I (New England Nuclear, Boston, MA). All reactions were performed at room temperature. The beads were rinsed with 100 mM TRIS (pH 7.0) and suspended in 200 μ l TRIS with Na-¹²⁵I. This mixture was incubated for 5 min. The dextran solution was then added (50 mg/100 μ l). After stirring for 30 min the solution was removed from the beads and 120 μ l of fresh sodium metabisulfite (Aldrich) was added. The product was purified by G10 Sephadex chromatography (Pharmacia Biotech, Piscataway, NJ) with PBS as eluent. The first peak fraction was collected and dialyzed against double-distilled water.

2.1.4. Diffusion of dextran through the arterial wall

We applied each dextran perivascularly from a hydrogel wrap that completely surrounded a segment of a rat carotid artery, and measured the rate at which drug traverses both native and wire-deendothelialized blood vessel walls. The calculated rate of drug flux and the transvascular concentration gradient enabled us to calculate the transmural resistance to transport. This resistance was resolved into the effective diffusivity in the arterial media, and the transendothelial resistance to transport using a multiple linear regression. The measurement of transmural drug transport was accomplished by following the concentration in the plasma after delivery; however, these levels were altered by redistribution of drug into non-plasma compartments and clearance by the kidney or liver. We therefore defined the systemic pharmacokinetic rate constants by which each drug moves out of the plasma (k_1), moves back into the plasma from the alternative compartment (k_2) and is cleared from the organism (k_{el}) (Fig. 1).

2.1.5. Determination of systemic pharmacokinetic rate constants

Sprague-Dawley rats (430–550 g) were anesthetized with an intraperitoneal injection of ketamine (60 mg/kg) and xylazine (15 mg/kg). Drug was administered as an intravenous bolus and the plasma levels were followed periodically for 4 h. Both carotid arteries were exposed and isolated via a midline cervical incision and each external carotid artery was cleaned of all adventitia and cannulated. Four ligatures were placed on each carotid artery using 4-0 silk (Roboz Surgical Rockville, MD) as follows: a loose proximal double loop on the common carotid artery, a loose double loop on the internal carotid artery, and on the external carotid artery a loose proximal single loop and a tight distal ligature. Flow was occluded in the common carotid by placing tension on the loose ligatures around the proximal common and internal carotid arteries. A small arteriotomy was made between the ligatures on each external carotid artery allowing insertion of a flanged polyethylene (PE-50) tube, which was secured in place by the proximal ligature on the external carotid artery. After both cannulas were inserted the loose ligatures were released and flow was restored.

For each compound, six rats received a bolus injection through one carotid arterial cannula, and periodic blood samples were withdrawn from the contralateral cannula. In addition, we wished to examine whether focal deendothelialization alters the systemic pharmacokinetic rate, perhaps from the release of inflammatory mediators. An additional set of bolus administration experiments was performed for each compound on another six rats whose left common carotid artery underwent gentle wire-deendothelialization [27]. Prior to insertion of the cannula, a flexible wire (5/0 monofilament surgical suture in PE10

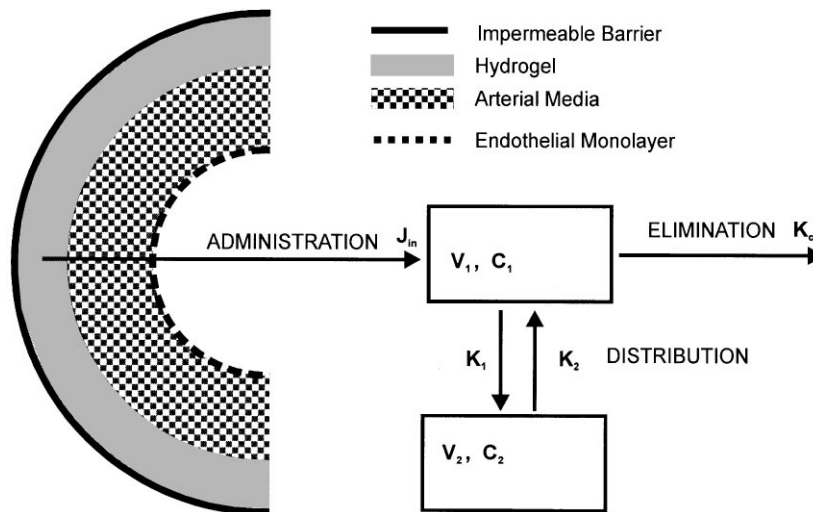


Fig. 1. Two-compartment model describing the redistribution and elimination of drug in the plasma. Drug is either delivered directly to the plasma (compartment 1) bolus, or from a perivascular release hydrogel wrap. The hydrogel resides within a Tygon collar that constrains drug release towards and across the artery (J_{in}). In either case, drug redistributes to an alternative compartment (2) according to the systemic rate constants k_1 and k_2 , and drug is cleared from compartment 1 through the kidneys or liver (k_{el}).

tubing) was introduced thrice through the arteriotomy, and withdrawn while turning the wire loop to denude the vessel of endothelium. Previous work has shown that this technique removes all of the endothelium within the isolated segment without any appreciable trauma to the underlying arterial media [27].

At the start of all bolus administration experiments 0.9 ml of labeled dextran in sterile normal saline was injected through the catheter into the carotid artery, and the catheter lumen was then flushed with 1 ml saline. At regular intervals over 4 h, blood was sampled (0.35–0.50 ml every 15–30 min) from the contra-lateral common carotid artery, and placed into 1.5 ml Eppendorf tubes. The volume in the PE50 tube itself was assumed to be negligible compared to the volume of the sample. The blood samples were centrifuged at 12 000 g for 10 min and 30 μ l of plasma samples were assayed for 125 I-dextran content using a Crystal Plus Multi detector RIA System 5400 series (Packard, Downers Grove, IL). The injected drug solution was also assayed for 125 I-dextran content.

2.1.6. Transmural transport measurements

Sprague Dawley rats were anesthetized and both carotid arteries were exposed, cleaned of all adventitia and cannulated as above. Drug was delivered to the perivascular surface of one of the arteries from a hydrogel wrap formed by cross-linking a prepolymer solution using a photoreactive technique [8]. The prepolymer consisted of a backbone of polyethylene glycol diacrylate 8 kDa (Focal Inc, Lexington, MA). This prepolymer was dissolved in 90 mM triethanolamine (30% wt/wt, Mallinckordt) to which *N*-vinylpyrrolidone (VP, 2 μ l/ml,

Aldrich) and 125 I-dextran (30 μ Ci/ml) were added. The concentration of the labeled dextran in the gel was measured as the average of samples taken from the prepolymer solution prior to polymerization and from the polymerized hydrogel after the experiment. In all experiments the concentration of the gel was nearly identical to the prepolymer solution indicating that the perivascular concentration was constant throughout each experiment.

The perivascular hydrogel release devices were formed in situ at the initiation of the experiment. Eosin Y (20 μ g/ml, Sigma Chemical Co (St. Louis, MO)) was added to dextran containing prepolymer solution and this mixture was injected (0.4–0.5 ml) into a Tygon collar mold (0.25" ID, 0.3125" OD) that surrounded the artery. Spacers made from short segments of smaller Tygon tubes were placed at both ends of the outer tube and held the artery in line with the center of the cylindrical mold. The prepolymer was photopolymerized with xenon fiber light source (488–514 nm, 70 mW/cm², ILC Technology) within 30 s of injection into the mold. The ends of the collar were photopolymerized first to prevent leakage of prepolymer out of the mold. The Tygon mold and spacers were left in place forming a barrier, which prevented drug from being absorbed by extra-arterial capillaries and lymphatics. The plasma levels of dextran were measured periodically through the cannula in the contralateral external carotid artery and assayed for 125 I-dextran concentration in a gamma counter. Each compound was delivered to the perivascular surface of six arteries that were left intact and to six arteries that were wire deendothelialized as above.

At the end of the experiment, the animals were sacrificed by an over dose of ketamine and xylazine. The collars were removed and assayed for drug concentration. The rats were perfused clear with lactated ringers and fixed at a pressure of 120 mmHg with 10% buffered formalin (Sigma) through the ipsilateral cannula to the drug delivery. The arteries were removed and paraffin embedded. The artery was sectioned from one end to the other and histologic samples were stained with hematoxylin and eosin from sections taken every 0.5 mm along the length (L) [28]. The circumference (P) and arterial medial thickness (l_{med}) of each section was measured with image analysis software (NIH Image) and average values for each artery were calculated from all of the histologic sections [28].

3. Data analysis and model fitting

3.1. Systemic pharmacokinetics

The systemic pharmacokinetic parameters (k_1, k_2, k_{cl}) were determined from the serum dextran levels following bolus administration. Data were analyzed using a two-compartment model and fit to the following equation with a non-linear regression algorithm using Kaleidagraph 3.0.1 (Fig. 1) [29].

$$C_1(t) = A_1 e^{\lambda_1 t} + \hat{A}_2 e^{\lambda_2 t} \quad (1)$$

The coefficients and exponents were then used to calculate the systemic pharmacokinetic rate constants k_1, k_2 , and k_{cl} [29]:

$$k_2 = \frac{-(\lambda_2(A_1/A_2) + \lambda_1)}{(A_1/A_2) + 1} \quad (2)$$

$$k_{cl} = \frac{\lambda_1 \lambda_2}{k_2} \quad (3)$$

$$k_1 = -(\ddot{e}_1 + \ddot{e}_2 + k_2 + k_{cl}) \quad (4)$$

3.2. Transmural transport

Using these systemic pharmacokinetic parameters, we fit the plasma concentration measurements, $C_1(t)$, with the following equation which is derived from the two-compartment model, and effectively corrects these measurements for systemic clearance and redistribution. In this way we determined the true transmural transport of drug, J_{in} [29]:

$$C_1(t) = \frac{J_m}{V_1 K_{cl}} \left[\frac{G}{1-G} e^{\lambda_1 t} - \frac{1}{(1-G)} e^{\lambda_2 t} + 1 \right] \quad (5)$$

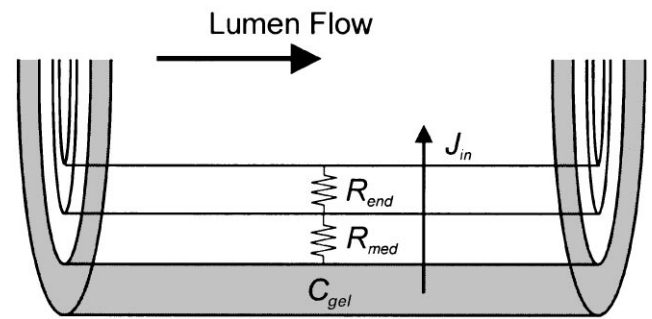


Fig. 2. The transmural transport is modeled as one dimensional. The adventitia was stripped from each artery prior to drug administration from a photopolymerizable perivascular hydrogel. The arterial media and the endothelium each exert a superimposable resistance to transarterial transport (J_{in}).

where

$$G = \frac{(K_{cl} + \lambda_2)}{(K_{cl} + \lambda_1)} \quad (6)$$

where V_1 is the volume of compartment one (Fig. 1) and assumed to be the plasma volume and estimated as 6% of rat body weight. The transmural resistance to transport (R_{tot}) was calculated, by analogy to Ohm's Law, in each experiment as

$$R_{tot} = C_{gel} - C_1 / (J_{in} / PL) \quad (7)$$

where L is the length of the artery, P is the perimeter of the lumen and C_{gel} is the average concentration of the hydrogel drug delivery device. The arterial wall was modeled as two concentric cylinders, each exerting resistance to transmural drug transport (Fig. 2), one from the media (R_{med}) and one from the endothelial monolayer (R_{end}), such that

$$R_{tot} = R_{med} + R_{end} \quad (8)$$

We assumed the resistance of the hydrogel to be negligible as the concentration of the perivascular (C_{gel}) was constant throughout the experiment, indicating that significant concentration gradients did not arise in the gel, and prior work has shown that solutes diffuse through these materials much faster than through tissues [30]. Thus, by analogy to Ohm's law, the potential difference for diffusive mass transfer is the product of the flux and the series sum of the resistances.

$$C_{gel} - C_1 = \left[\frac{J_{in}}{PL} \right] (R_{med} + b_{end} R_{end}) \quad (9)$$

The coefficient of R_{end} (b_{end}) was 0 after denuding injury and 1 with an intact native artery [28]. A linear relationship was assumed between the arterial wall resistance and its thickness such that

$$R_{med} = l_{med} / D_{med} \quad (10)$$

where l_{med} is the average medial thickness and D_{med} is the effective diffusivity of each compound in the arterial media. Rearrangement of Eq. (8) allows the unknowns D_{med} and R_{end} to be determined by multiple linear regression:

$$PL(C_{\text{gel}} - C_1)/J_{\text{in}} = l_{\text{med}}/D_{\text{med}} + b_{\text{end}}R_{\text{end}}. \quad (11)$$

Statistics. Data are expressed as mean \pm standard deviation. Statistical Significance was assessed by ANOVA and achieved for $p < 0.05$.

4. Results

4.1. Dextran preparation

To examine the individual roles of molecular weight and charge on transport we prepared four different size neutral and inert dextrans, and sulfated or aminated dextrans at one molecular weight (40 kDa). All reactions produced pure compounds with minimal increase in GPC determined molecular weight or polydispersity. Neutral dextrans were conjugated with 0.7–1.50 tyramine molecules per dextran (UV absorption $\lambda_{\text{max}} = 275$ nm) in good yields (55–80%). Elemental analysis revealed that the sulfated compounds contained 0.9 sulfate groups per glycosidic ring (S, 17.79%), and isoelectric focusing gel chromatography showed that the pI was less than 3. However, up to 35% of the rings had been conjugated with DMEDA, and 10% were conjugated to both tyramine and DMEDA. The pI of amino dextrans was 8.8–10. All model compounds were radiolabeled with Na^{125}I successfully to a specific activity of 0.005–0.01 $\mu\text{Ci}/\mu\text{g}$, and delivered intravenously and perivascularly in a rat model.

4.2. Transport: systemic pharmacokinetics

The elimination of intravenously delivered neutral dextrans as a function of molecular weight fit a linear bi-exponential decay (Fig. 3). Six independent experiments were performed. For clarity only the clearance curves for bolus administration with native arteries are shown, as curves obtained with wire deendothelialized rats were nearly identical. Low molecular weight dextrans cleared quickly, with less than 10% of the compound residing in the blood 30 min after injection. In contrast, more than 40% of the initial 282-kDa dextran injected remained in the circulation after 30 min. Clearance rate constants were calculated from the fit of these data using Eq. (1) (Table 1). Both k_1 and k_{el} are greatest with smaller and positively charged compounds. For most compounds there was not a statistical difference between the systemic rate constants obtained in rats with native and focally denuded carotid arteries. These systemic rate constants obtained with native arteries were

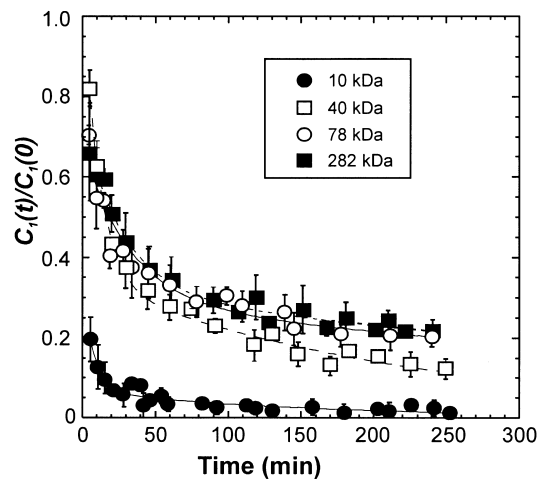


Fig. 3. Normalized clearance profiles for various sizes of ^{125}I -dextran after bolus administration to the carotid artery. (avg \pm SD, $n = 6$). The concentration in the plasma is (compartment 1) is normalized by the initial concentration derived from the biexponential curve fit (Eq. (1)). The systemic pharmacokinetic rate-constants k_1 , k_2 , and k_{el} were determined from this fit using Eqs. (2)–(4). These rate constants were then used to correct plasma drug concentration measurements following perivascular delivery Eq. (5). Data for dextran sulfate and dextran amine are not shown.

Table 1

Systemic pharmacodynamic rate constants as calculated from the fit of the intravascular bolus injection data (Fig. 3, Eq. (1)) ($\times 0.01 \text{ min}^{-1} \pm \text{SD}$, $n = 6$)

| | k_1 | k_2 | k_{el} |
|-----------------|-----------------|-----------------|-----------------|
| <i>MW</i> | | | |
| 10 K | 9.13 ± 1.43 | 2.87 ± 0.79 | 4.89 ± 1.09 |
| 40 K | 4.37 ± 0.56 | 3.09 ± 0.56 | 1.24 ± 0.34 |
| 78 K | 3.10 ± 0.82 | 3.51 ± 0.44 | 0.51 ± 0.03 |
| 282 K | 3.11 ± 1.1 | 3.23 ± 1.01 | 0.36 ± 0.07 |
| <i>Charge</i> | | | |
| DS 40 kDa | 1.61 ± 0.55 | 5.81 ± 2.35 | 0.52 ± 0.09 |
| DMEDA-DX 40 kDa | 4.42 ± 1.17 | 3.01 ± 0.49 | 2.52 ± 1.14 |

used in determining J_{in} (Eq. (5)) from serum samples collected with perivascular delivery to native arteries, and likewise for wire deendothelialized arteries.

4.3. Transport: local

To demonstrate the importance of endothelial resistance in transmural drug transport, normalized plasma concentrations of 78 kDa neutral dextrans are shown for native and denuded arteries following local perivascular application (Fig. 4). The total transmural resistance to transport is shown for native and deendothelialized arteries as a function of molecular weight (Fig. 5a) and charge (Fig. 5b). At low molecular weights (< 40 kDa) and for positively charged compounds, the transmural

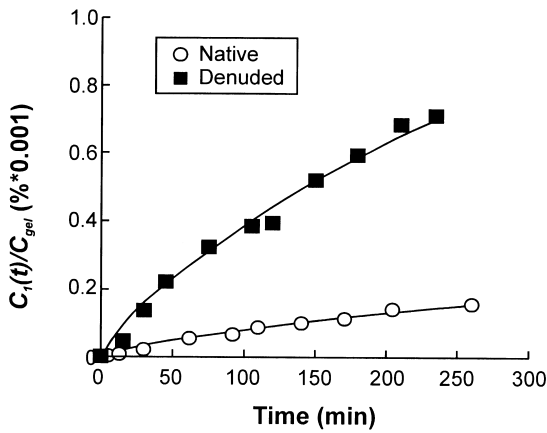


Fig. 4. Sample plasma concentration over time normalized by the concentration in the hydrogel following perivascular delivery of 125 I-dextran 78 kDa to native and deendothelialized carotid arteries. The curve fit lines were generated by Eq. (5).

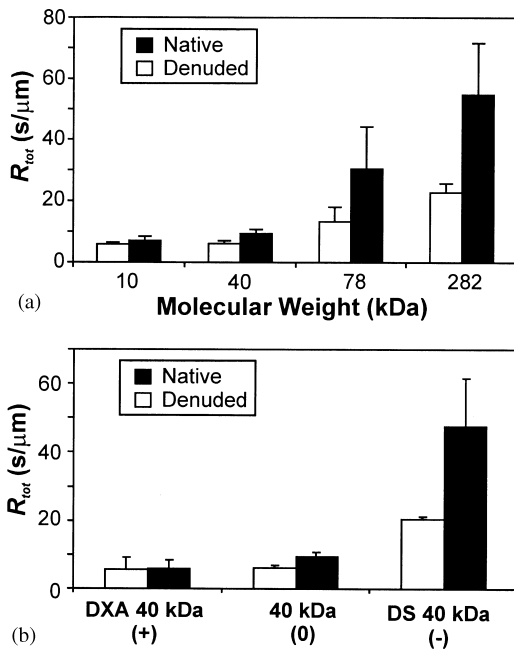


Fig. 5. The total resistance to transmural transport (R_{tot}) of dextrans as a function of molecular weight (a) and charge (b) as calculated by Eq. (7) (avg \pm SD, $n = 6$).

resistances are indistinguishable for native and denuded arteries. As the molecular weight is increased, or the charge becomes more negative, the total resistance increases and the difference between native and deendothelialized vessels became more pronounced. For example, with DS 40 kDa and with 78 and 282 kDa neutral dextrans the total resistance with native arteries was greater than twice as much as when the endothelium was removed.

We calculated the effective diffusivity in the arterial media (D_{med}) and the transendothelial resistance to trans-

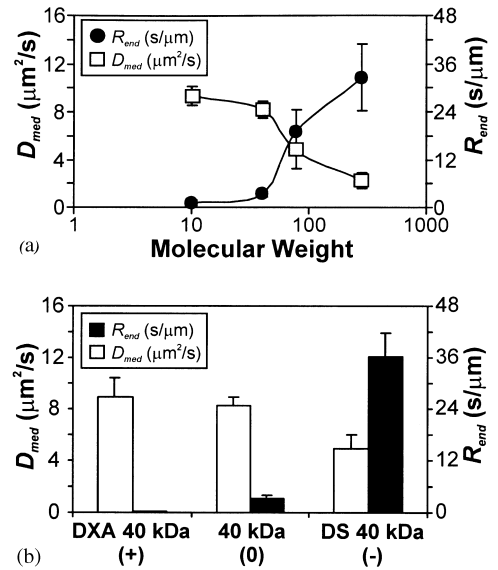


Fig. 6. The effective diffusivity in the arterial media (D_{med}) and the transendothelial resistance to transport (R_{end}) as a function of dextran MW (a) and charge (b) (avg \pm SD, $n = 6$). Note the different scales used.

port (R_{end}) using arterial morphometric measurements and multiple linear regression of the total resistance data in the form of Eq. (11) (Fig. 6). The effective diffusivity in the arterial media fell with molecular weight; gradually from 10 to 40 kDa, and then more sharply above 40 kDa, such that the effective diffusivity at 10 kDa was 4.1 fold greater than at 282 kDa. The transendothelial resistance increased with molecular weight, only slightly from 10 to 40 kDa, and then much more dramatically above 40 kDa such that this resistance increased 27.8 fold from 10 to 282 kDa. The effective medial diffusivity of cationic and neutral dextrans were identical, but 39.8 and 44.4% higher than that of the anionic dextran sulfated dextrans. As the endothelial monolayer is more sensitive to molecular weight than arterial media, the endothelium is also more sensitive to charge. The transendothelial resistance was 19.5 fold higher for neutral than positively charged dextran, and the resistance with the negatively charged dextran sulfate was 10.9 fold higher than its neutral counterpart.

5. Discussion

The complex trilaminar architecture of the blood vessel wall would naturally lead one to believe that there are substantial barriers to the entry and transport of macromolecules, and that drugs with one set of physicochemical properties may be handled entirely differently by the artery than drugs with radically different attributes. An appreciation of how the arterial wall differentially deals with each compound would be of great value in understanding repair and signaling, and in

developing arterial delivery systems. If these findings could be generalized they might predict the fate of a released drug without the need for experiments for every scenario, drug and arterial state imagined. We examined how changes in drug properties impact the most relevant vascular pharmacokinetic parameters. Molecular weight and charge were examined in particular, as these physico-chemical properties have been demonstrated to influence the transport of solutes in tissues *in vivo*, and gels and matrices *in vitro* [31–34]. Their effect on dextran transport was quantified in terms of the effective medial diffusivity, and the transendothelial resistance to transport, as these parameters have been measured *in vitro* using heparin as a model vasoactive agent [11,28]. Neutral dextrans that varied in molecular weight (10–282 kDa), and chemically modified dextrans of a single molecular weight that varied in charge from cationic dextran sulfate to anionic dextran amine (DMEDA), were released perivascularly to native or wire deendothelialized rat carotid arteries from photopolymerized PEG-diacrylate hydrogels.

The transarterial rate of drug transport (J_{in}) was determined from sampled plasma drug levels, histologically determined vascular dimensions. For many of the compounds tested the clearance by the kidneys and redistribution to the extravascular compartment was significant. We therefore corrected the measured plasma drug levels for these events. Additional experiments were performed for each compound in which drug was injected and the plasma levels were followed over four hours (Fig. 3). The plasma levels in these bolus delivery experiments showed a characteristic biexponential decay that allowed us to apply a two-compartment systemic pharmacokinetic model (Fig. 1) to determine the clearance (k_{cl}) and the redistribution constants (k_1, k_2 , Eqs. (1)–(4), Table 1) [29]. These constants were applied to the perivascular release data to calculate the true transarterial transport (Eq. (5), J_{in}) used in the multiple linear regression analysis (Eq. (11)).

5.1. Systemic pharmacokinetics

The normalized concentration–time curves obtained from the bolus administration experiments were fit to a linear bi-exponential equation to determine the rate constants k_1, k_2 and k_{cl} for the various compounds (Table 1). The initial decay represents the redistribution from the plasma to the second compartment, which physically may represent some combination of extravascular fluid, intracellular fluid and fat. The rate constant k_1 decreased with molecular weight and negative charge as compounds of smaller molecular weights and more positive charge redistribute from the vasculature faster, presumably because of the lesser steric hindrance and more favorable electrostatic interactions. The second decay in the biexponential represents the clearance from

the organism (k_{cl}). Extravasation of macromolecules after intravenous administration in rats is primarily governed by their hepatic uptake and urinary excretion [35]. The kidneys play an important role in the disposition of macromolecules of MW less than 50 kDa because of their susceptibility to glomerular filtration and urinary excretion. However, anionic macromolecules show significantly slower rates of clearance compared with neutral and cationic dextrans, which are taken up by the liver based on adsorption of the negatively charged cell surface [35]. Our data show that clearance (k_{cl}) decreases with molecular weight and negative charge, likely from the size and charge-selective barrier in the renal glomerulus. The systemic pharmacokinetic constants (k_1, k_2, k_{cl}) were statistically indistinguishable when measured in native and deendothelialized arteries. The identity of these parameters implies that the focal injury did not release cytokines or factors that might have altered vascular permeability or excretion, and that the measured constants could be applied equally well to the perivascular release data taken with both native and denuded arteries.

5.2. Local arterial pharmacokinetics

To eliminate the impact of slight variability in drug loading in the hydrogel, we normalized the transarterial transport rate (J_{in}) by the concentration gradient across the artery ($C_{gel} - C_1$) enabling us to determine the total transarterial resistance to drug transport (R_{tot}) for each perivascular release experiment (Eq. (7), Fig. 5). The transarterial transport of drug was always greater, and the total resistance lower when the endothelium was removed than when it was left intact, implying that this thin monolayer imparts a significant resistance to drug transport *in vivo*. We modeled the arterial wall as two concentric cylinders, representing the media and the endothelium, each imparting a separate resistance to drug transport to the one-dimensional transmural flow of drug from the perivascular source (Fig. 2). As the average concentration of the perivascular gel (C_{gel}) did not change over the course of the experiment, significant concentration gradients did not arise in the gel, and the resistance of the hydrogel could therefore be neglected in our analyses. In addition we have shown that compounds diffuse through similar hydrogels much faster than through tissues [30]. The hydrogel does not affect transmural transport as the concentration nearest the tissue always has a concentration of drug that is similar to the average in the whole device. For each compound we determined the corrected transmural mass transfer rate of drug (J_{in}) using the systemic pharmacokinetic rate constants (k_1, k_2, k_{cl}) and Eq. (5). We combined these data with the length (L) and perimeter (P) of the artery and the medial thickness (l_{med}) measured in the histologic sections and determined D_{med} and R_{end} using a multiple linear regression of Eq. (11).

As the molecular weight of the drug increased from 10 to 282 kDa, D_{med} fell four-fold (Fig. 6a). This trend was nonlinear as the diffusivity in the media fell rapidly as the size of the compounds of molecular weight larger than 40 kDa. The transendothelial resistance increased dramatically with molecular weight (Fig. 6a). The resistance was negligible to 10 kDa compounds, low for 40 kDa dextrans, and rose sharply for larger molecular sizes. At low molecular weights the resistance to transport through the arterial media dominates the motion of the compound, while at higher molecular weights the endothelium plays a larger and eventually dominant role in governing local vascular pharmacokinetics. The neutral and positively charged dextrans have statistically indistinguishable effective diffusivities in the arterial media (D_{med}), while that of the negative dextran sulfates were half of these values. In the endothelial monolayer these charged interactions are even more dramatic. R_{end} for the neutral compounds was 19-fold higher than for the positively charged compounds of similar molecular weight (Fig. 6b). Likewise, R_{end} for the negative dextran sulfates were 11-fold higher than for its neutral counterpart. Both the arterial interstitium and the gap junctions of the endothelial monolayer contain fixed negative charges in the form of glycosaminoglycans that induce differential partitioning of compounds with different charges. Positively charged compounds partition to a greater extent than those that are neutral, which partition more so than negatively charged solutes. This increased partitioning of positive compounds leads to larger concentration gradients within the substrate and hence faster diffusive transport. Conversely, the fixed negative charges repel negative solutes causing low partitioning and low concentration gradients and diminished transport. The transendothelial resistance to transport is far more sensitive to charge than the effective diffusivity in the arterial media, likely the result of the higher density of fixed negative charges in the endothelium from greater concentrations of glycosaminoglycans in the gap junctions. Although the endothelium comprises 1–3% of the thickness of the rat carotid artery, its effect on perivascular transport is dominant with negative and large compounds.

The most direct prior evidence that charge plays a dominant role in macromolecular transport is from studies in the renal glomerulus [36]. Cationic DMEDA-dextrans are cleared more rapidly than neutral dextrans and dextran sulfate, as they are neither secreted nor reabsorbed by the renal tubules to any measurable extent [36,37]. The cationic dextrans are cleared with enhanced filtration that results from the significant electrostatic interaction between circulating charged macromolecules and the negatively charged components of the glomerular capillary wall [33]. It has been shown also that the glomerular filtration of cationic DEAE-dextran and cationic BSA is enhanced compared to

that of their uncharged counterparts, whereas that of anionic BSA and carboxymethyl dextran is impaired. These results support the notion of the glomerular capillary wall as a size and charge-selective barrier and these same mechanisms likely apply to the arterial interstitium and the intercellular spaces of the endothelial monolayer.

6. Conclusions

The transmural flux of any drug through the arterial wall, J_{in} , can be calculated in vivo after correction with systemic pharmacokinetic rate constants. Using a variety of dextrans, this flux was highly dependent on molecular size and charge as such parameters controlled the extent to which the drug distributed from the vascular to the tissue compartments. Endothelial resistance increased, whereas medial effective diffusivity decreased, with dextran molecular weight. These results suggest that on one hand, low molecular weight compounds rapidly traverse the arterial wall with the endothelium posing as a minimal barrier. On the other hand, larger molecules slowly traverse the arterial wall with the intact endothelium posing as a substantial barrier. With these findings we can now predict deposition and distribution of locally released vasoactive compounds based upon standard chemical properties, such as molecular weight and charge.

Acknowledgements

This study was supported in part by grants from the National Institutes of Health (GM/HL 49039, HL 60407), the Burroughs-Wellcome Fund in Experimental Therapeutics, and the Whitaker Foundation in Biomedical Engineering. Elazer Edelman is an Established Investigator of the American Heart Association.

References

- [1] Ip JH, Fuster V, Badimon L, Badimon J, Taubman MB, Chesebro JH. Syndromes of accelerated atherosclerosis: role of vascular injury and smooth muscle proliferation. *J Am Coll Cardiol* 1990; 15:1667–87.
- [2] Lidner V, Majack RA, Reidy MA. Basic fibroblast growth factor stimulates endothelial regrowth and proliferation in denuded arteries 1990;85:2004–8.
- [3] Edelman ER, Adams DA, Karnovsky MJ. Effect of controlled adventitial heparin delivery on smooth muscle cell proliferation following endothelial injury. *Proc Natl Acad Sci USA* 1990; 87:3773–7.
- [4] Okada T, Bark DH, Mayberg MR. Local anticoagulation without systemic effect using a polymer heparin delivery system. *Stroke* 1988;19:1470–6.

- [5] Lambert T, Dev V, Rechavia E, Forrester JS, Litvack F, Eigler NL. Localized arterial wall drug delivery from a polymer-coated removable metallic stent. Kinetics, distribution, and bioactivity of forskolin. *Circulation* 1994;90:1003–11.
- [6] Villa A, Guzman L, Chen W, Golomb G, Levy R, Topol E. Local delivery of dexamethasone for prevention of neointimal proliferation in a rat model of balloon angioplasty. *J Clin Invest* 1994; 93:1243–9.
- [7] Rogers C, Karnovsky MJ, Edelman ER. Inhibition of experimental neointimal hyperplasia and thrombosis depends on the type of vascular injury and the site of drug administration. *Circulation* 1993;88:1215–21.
- [8] Hill-West JL, Chowdhury SM, Slepian MJ, Hubbell JA. Inhibition of thrombosis and intimal thickening by in situ photopolymerization of thin hydrogel barriers. *Proc Nat Acad Sci* 1994;91:5967–71.
- [9] Slepian MJ, Campbell PK, Berrigan K, Roth L, Massia SP, Wesselcouch E, Ron E, Mathiowitz E, Jacob J, Chickering D, Philbrook M. Biodegradable endoluminal polymer layers provide sustained transmural heparin delivery to the arterial wall in vivo. *Circulation* 1994;90(abstract):I-20.
- [10] Slepian MJ. Polymeric endoluminal paving: evolving therapeutic methods extending the spectrum of local endovascular interventions. In: Liermann D, editor. *Stents: state of the art and future developments*. Morin Heights, Canada: Polyscience Publications Inc., 1995. p. 339–55.
- [11] Lovich MA, Philbrook M, Sawyer S, Wesselcouch E, Edelman ER. Arterial heparin deposition: role of diffusion convection, and extravascular space. *Am J Physiol* 1998;275:H2236–42.
- [12] Edelman ER, Nugent MA, Karnovsky MJ. Perivascular and intravenous bFGF administration: vascular and solid organ deposition. *Proc Nat Acad Sci USA* 1993;30:1513–7.
- [13] Edelman ER, Lovich MA. Drug delivery models transported to a new level. *Nature Biotechnol* 1998;16:146–7.
- [14] Bratzler RL, Chisolm GM, Colton CK, Smith KA, Zilversmit DB, Lees RS. The distribution of labeled low-density lipoproteins across the rabbit thoracic aorta in vivo. *Atherosclerosis* 1977; 28:289–307.
- [15] Duncan LE, Buck K, Lynch A. Lipoprotein movement through canine aortic wall. *Science* 1963;142:972–3.
- [16] Fry DL, Cornhill JF, Sharma H, Pap JM, Mitschelen J. Uptake of low density lipoprotein, albumin, and water by deendothelialized in vitro minipig aorta. *Arteriosclerosis* 1986;6:475–90.
- [17] Scott PJ, Hurley PJ. The distribution of radio-iodinated serum albumin and low-density lipoprotein in tissues and the arterial wall. *Arteriosclerosis* 1971;11:77–103.
- [18] Adams CWM, Morgan RS, Bayliss OB. The differential entry of [¹²⁵I]albumin into mildly and severely atheromatous rabbit aortas. *Arteriosclerosis* 1970;11:119–24.
- [19] Caro CG, Ebel W, Laver-Rudich Z, Liron N, Meyer F. Steady albumin transport in the rabbit common carotid artery. *Arteriosclerosis* 1979;289:497–511.
- [20] Bratzler RL, Chisolm GM, Colton CK, Smith KA, Zilversmit DB, Lees RS. The distribution of labeled albumin across the rabbit thoracic aorta in vivo. *Circ Res* 1977;40:182–90.
- [21] Fry DL. Effect of pressure and stirring on in vitro aortic transmural ¹²⁵I-albumin transport. *Am J Physiol* 1983;245:H977–91.
- [22] Lee MK, Lander AD. Analysis of affinity and structural selectivity in the binding of proteins to glycosaminoglycans: development of a sensitive electrophoretic approach. *Proc Natl Acad Sci USA* 1991;88:2768–72.
- [23] San Antonio JD, Slover J, Lawler J, Karnovsky MJ, Lander AD. Specificity in the interactions of extracellular matrix proteins with subpopulations of the glycosaminoglycan heparin. *Biochemistry* 1993;32:4746–55.
- [24] Ricketts C. A synthetic analogue of heparin. *Biochem J* 1952; 51:129–33.
- [25] Bernstein A, Hurwitz E, Maron R, Arnon R, Sela M, Wilchek M. Higher antitumor efficacy of daunomycin when linked to dextran: in vivo and in vitro studies. *J Natl Cancer Inst* 1978;60:379–84.
- [26] Zhao H, Heindel ND. Determination of degree of substitution of formyl groups in polyaldehyde dextran by the hydroxylamine hydrochloride method. *Pharm Res* 1991;8:400–2.
- [27] Fingerle J, Au YPT, Clowes AW, Reidy MA. Intimal lesion formation in rat carotid arteries after endothelial denudation in absence of medial injury. *Arteriosclerosis* 1990;10:1082–7.
- [28] Lovich MA, Edelman ER. Mechanisms of transmural heparin transport in the rat abdominal aorta after local vascular delivery. *Circ Res* 1995;77:1143–50.
- [29] Greenblatt DJ, Kock-Weser J. Drug therapy. *Clinical Pharmacokinetics* (first of two parts). *N Engl J Med* 1975;293:702–5.
- [30] Lovich MA, Edelman ER. Computational simulations of local vascular heparin deposition and distribution. *Am J Physiol* 1996; 271:H2014–24.
- [31] Johnson EM, Berk DA, Jain RK, Deen WM. Diffusion and partitioning of proteins in charged agarose gels. *Biophys J* 1995; 68:1561–8.
- [32] Jain RK. Transport of Macromolecules in tumor microcirculation. *Biotechnol Prog* 1985;1:81–94.
- [33] Deen WM, Bohrer MP, Brenner BM. Macromolecular transport across the glomerular capillaries: application of pore theory. *Kidney Int* 1979;16:353–65.
- [34] Deen WM, Satvat B, Jameieson JM. Theoretical model for glomerular filtration of charged solutes. 1980;238:F126–39.
- [35] Hashida M, Kato A, Takakura Y, Sezaki H. Disposition and pharmacokinetics of a polymeric prodrug of mitomycin C, mitomycin C-dextran conjugate, in the rat. *Drug Metab Dispos* 1984;12:492–9.
- [36] Chang RLS, Deen WM, Robertson CR, Brenner BM. Permselectivity of the glomerular capillary wall. III. Restricted transport of polyanions. *Kidney Int* 1975;8:212–8.
- [37] Chang RLS, Ueki IF, Troy JL, Deen WM, Robertson CR, Brenner BM. Permselectivity of the glomerular capillary wall to macromolecules. II. Experimental observations in the rat. *Biophys J* 1975;15:887–906.